The 8th KIAS Workshop (Nov 7, 2018)

Discovery of a New Fundamental Dictating Galaxy Cluster Evolution from Gravitational Lensing

- Fujita, Umetsu, Rasia, Meneghetti, Donahue et al. 2018a, *ApJ*
- Fujita, Umetsu, Ettori, Rasia et al. 2018b, ApJ
- Umetsu, Zitrin,Gruen et al. 2016, ApJ

Keiichi Umetsu, ASIAA, Taipei, Taiwan

Galaxy clusters as a sensitive probe of nonlinear structure formation

- Standard paradigm for structure formation: ΛCDM
  - Collisionless, cold dark matter
- Clusters offer fundamental tests of assumed DM properties:
  - DM density, $\rho(r|M)$ Umetsu+11, 14, 16
  - Splashback density steepening Umetsu+17
  - Splashback in phase space Okumura+18
  - Halo shape and alignments Umetsu+18
  - Substructure distribution Okabe+14
  - DM/galaxy/gas offsets Clowe+14

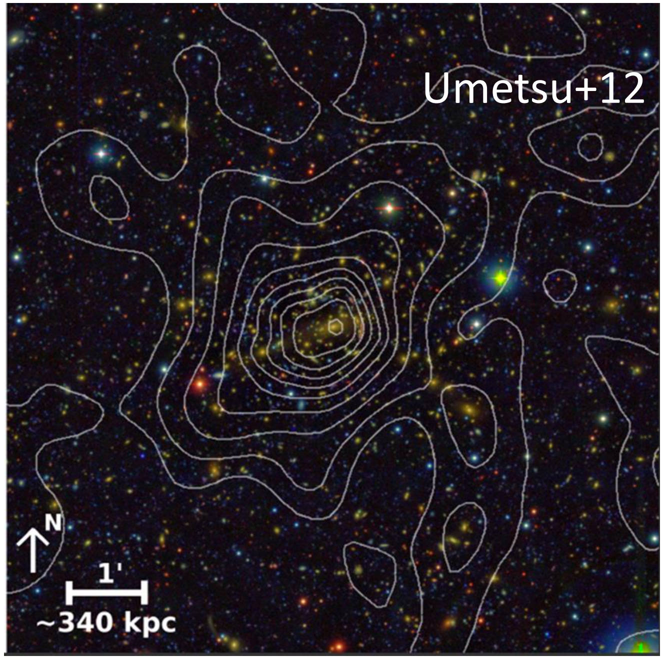

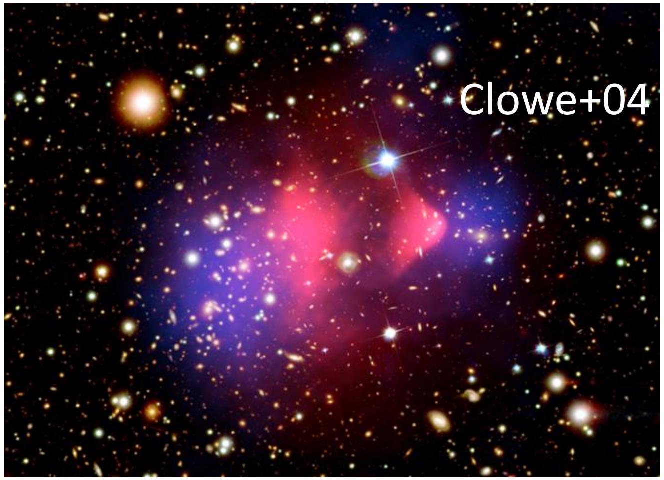

End-product of collisionless collapse in an expanding universe, $\rho(r|M)$

Quasi-equilibrium halos with

$$\frac{1}{2}\langle \ddot{I} \rangle = 2T - |W| - S \approx 0$$

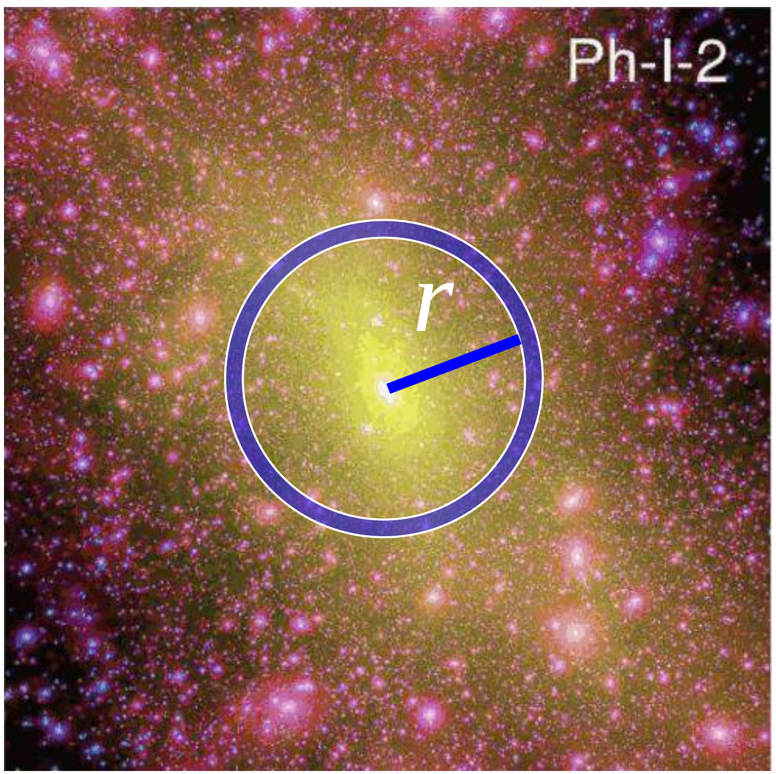

Navarro-Frenk-White (NFW) profile

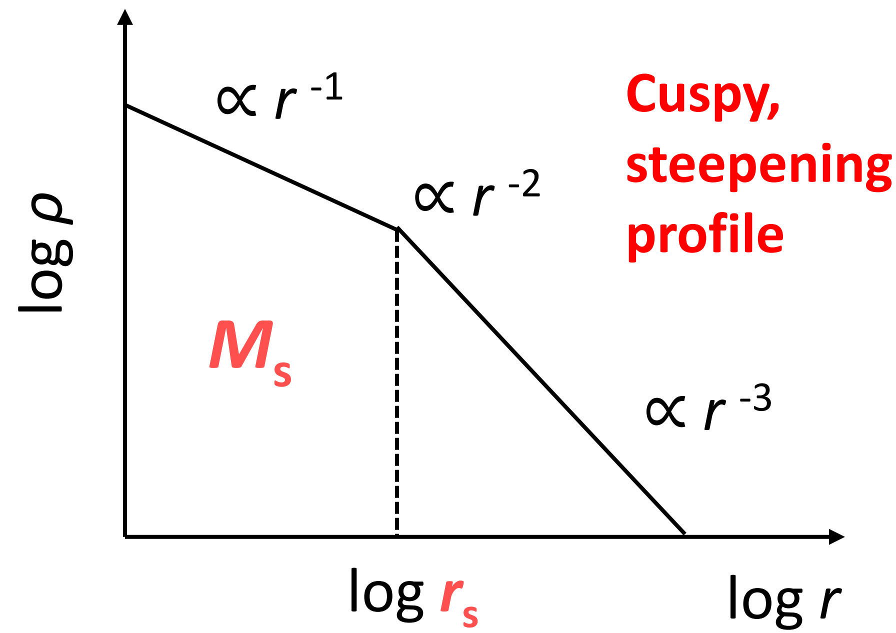

$$\boxed{\frac{d\ln\rho(r)}{d\ln r} = -2 \ @\ r = r_s}$$

$$\max(V_{\rm circ})\ @\ r \approx 2r_s$$

Cluster mass distribution—cuspy, NFW-like

~20 high-mass clusters with $\langle M_{200c} \rangle = 1.4 \times 10^{15} M_{sun}$ (CLASH survey)

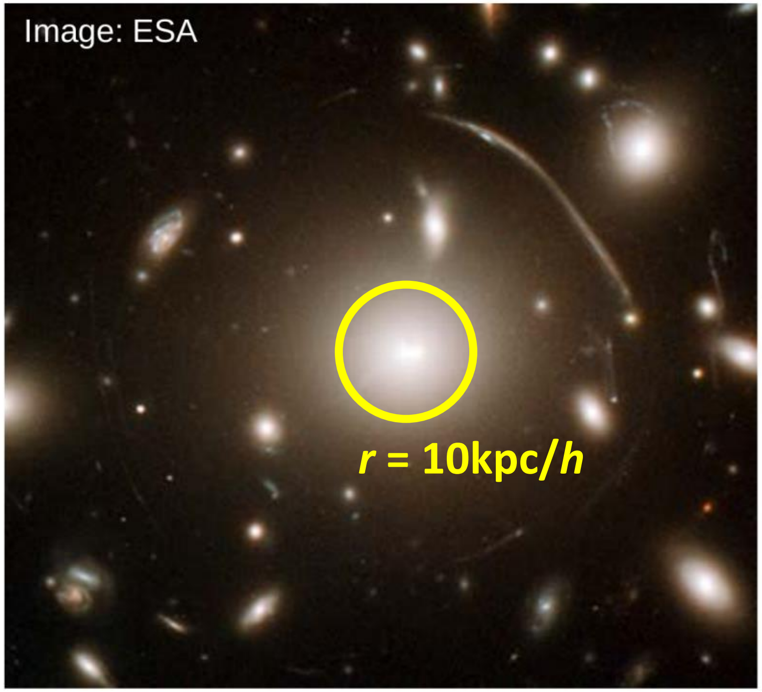

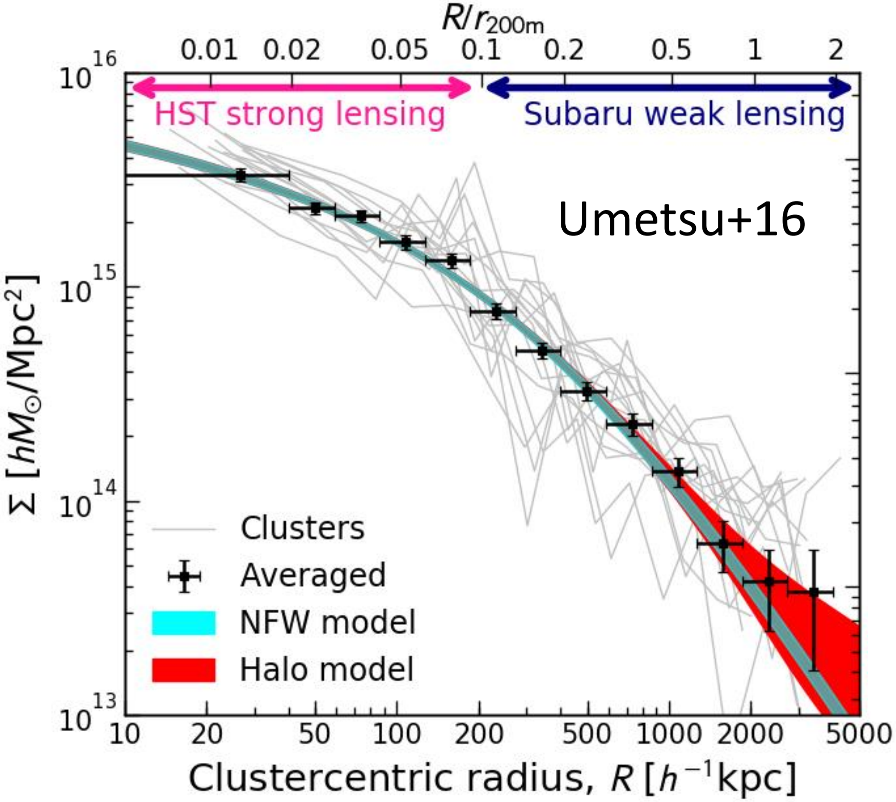

- Excellent agreement with CDM over 99% of radial range (r_{min}=40kpc/h)
- Innermost density slope: γ=0.9 (+0.2, -0.3) with $\rho(r) \sim r^{-\gamma}$ $(\gamma_{CDM} = 1)$
- Concentration c_{200c}=3.8 +/- 0.3 precisely matching the LCDM prediction
- Halo ellipticity 1-<b/a>=0.33+-0.07, consistent with LCDM (Umetsu+18)

Splashback steepening in cluster lensing data

R_Δ-rescaled joint fit

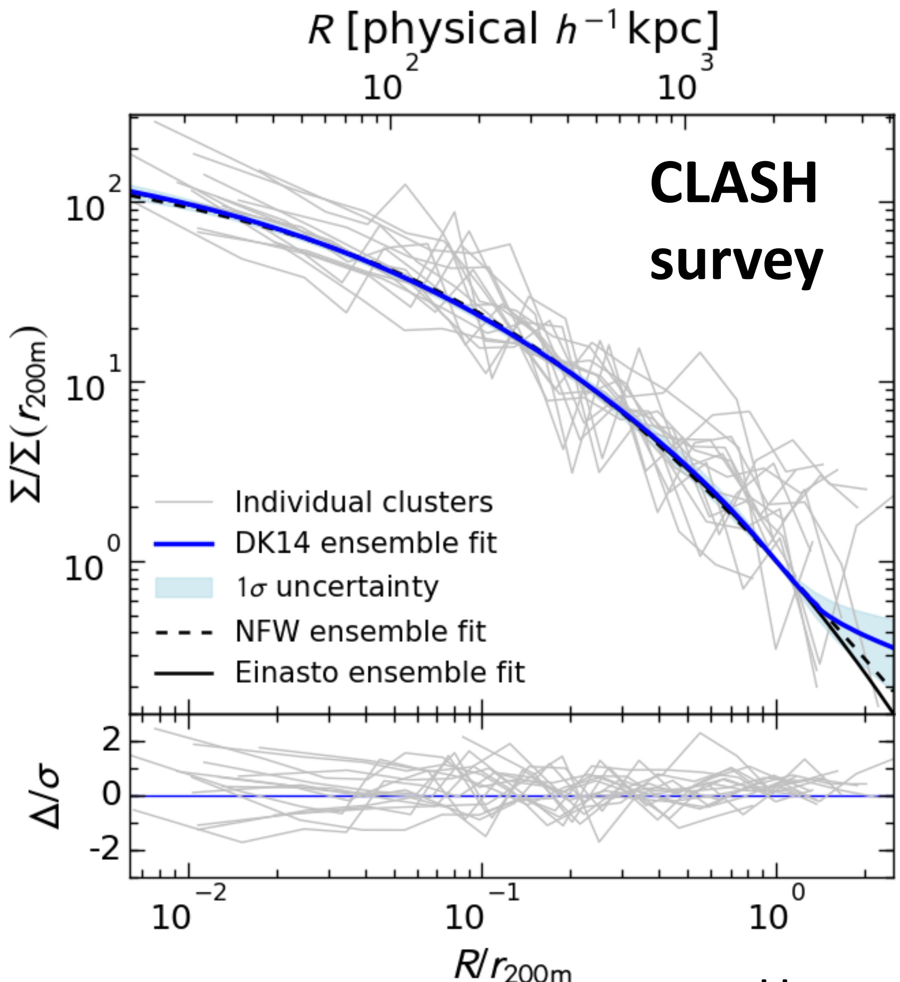

First lensing constraints on the splashback radius R_{sp}

$$R_{sp} / r_{200m} > 0.89\,(1\sigma)$$

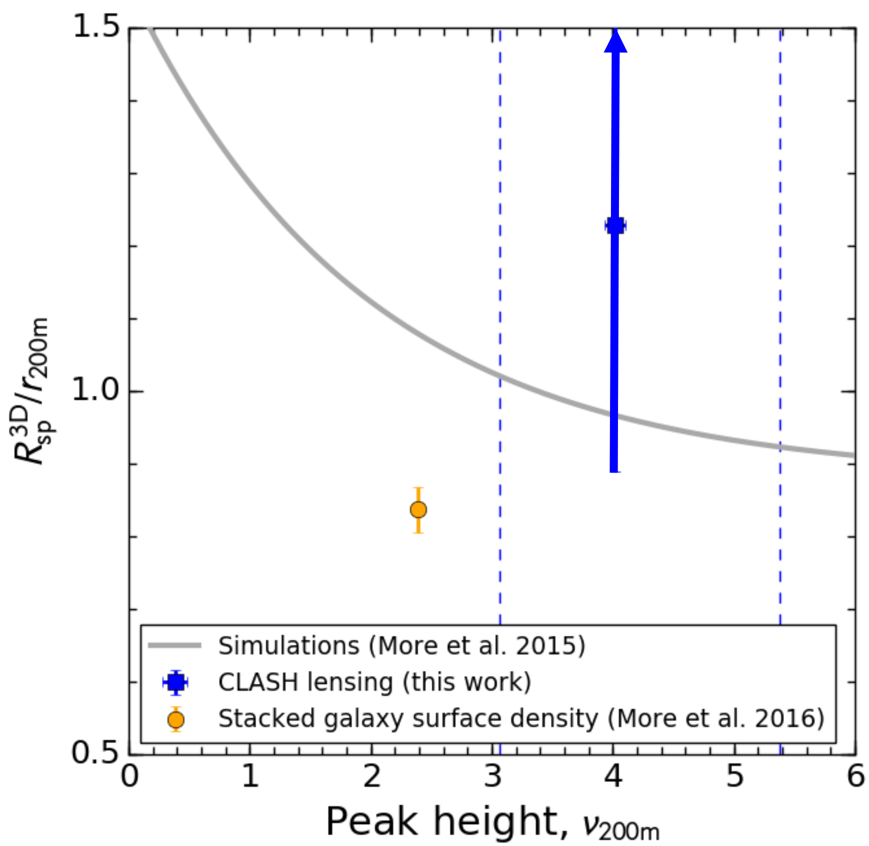

Umetsu & Diemer 2017, ApJ

How DM halos form and grow?

"Inside-out" growth scenario (ΛCDM)

- DM halos are assembled from the inside out (Wechsler+02, Zhao+03)
- Halo's internal structure reflects their growth history (Ludlow+13)

(1) **Fast-growth phase**

Inner region ($<r_s$) grows rapidly via massive major mergers

(2) **Slow-growth phase**

Halo outskirts ($> r_s$) gradually grow via smooth matter accretion from surroundings, without changing the inner potential significantly

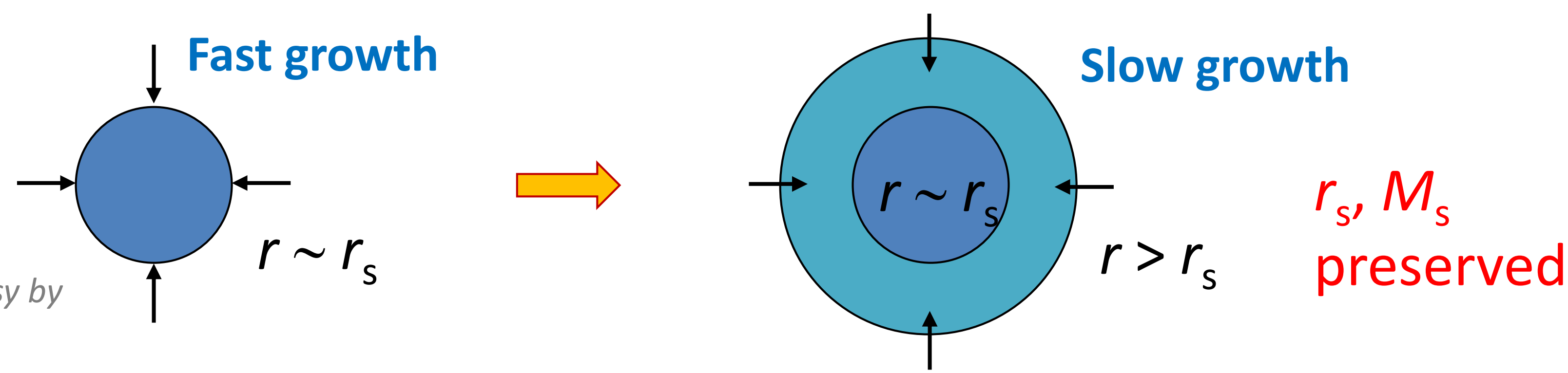

Figure courtesy by Y. Fujita

Key questions in this talk

How about real halos? → high-mass clusters ($M \sim 10^{15} M_{sun}$)

How about baryons? → hot gas (>80% of the cluster baryons)

- **Lensing observables**: halo's scale radius and mass (r_s, M_s), with $r_s \sim 0.2\, R_{sp} \sim$ 500kpc for high-mass clusters
- **Baryonic observable**: X-ray gas temperature, T_X

Are the DM and baryon halo parameters tightly coupled?

  - ***If yes***: The hot gas was likely heated during the fast-growth phase (i.e., major mergers), and T_X was preserved in the subsequent slow-growth phase.

If so, **how do (M_s, r_s, T_X) correlate? What is the degree of scatter?**

Canonical predictions (e.g., virial equilibrium, Komatsu-Seljak pressure model):

$$T \propto f(c)\frac{M_s}{r_s} \sim \frac{M_s}{r_s}$$

Deep multi-wavelength data sets from the CLASH survey

High-resolution strong lensing & weak shear lensing analysis of all 25 CLASH clusters with deep 16-band *HST* ACS/WFC3 imaging (Zitrin+15, *ApJ*, 795, 163)

Wide-field weak-lensing shear & magnification analysis of 20 CLASH clusters with deep 5-6 band Subaru Suprime-Cam imaging (Umetsu+14, *ApJ*, 795, 163)

***HST*+Subaru-combined, strong-lensing, weak-lensing shear & magnification analysis** (Umetsu+16, *ApJ*, 821, 116)

X-ray analysis of all 25 CLASH clusters with deep *Chandra* and *XMM* X-ray imaging and spectroscopy (Donahue+14, *ApJ*, 797, 34)

Subaru/Suprime-Cam multi-color imaging for weak lensing shear & magnification

High-resolution space imaging with *HST* (ACS/WFC3) for strong lensing

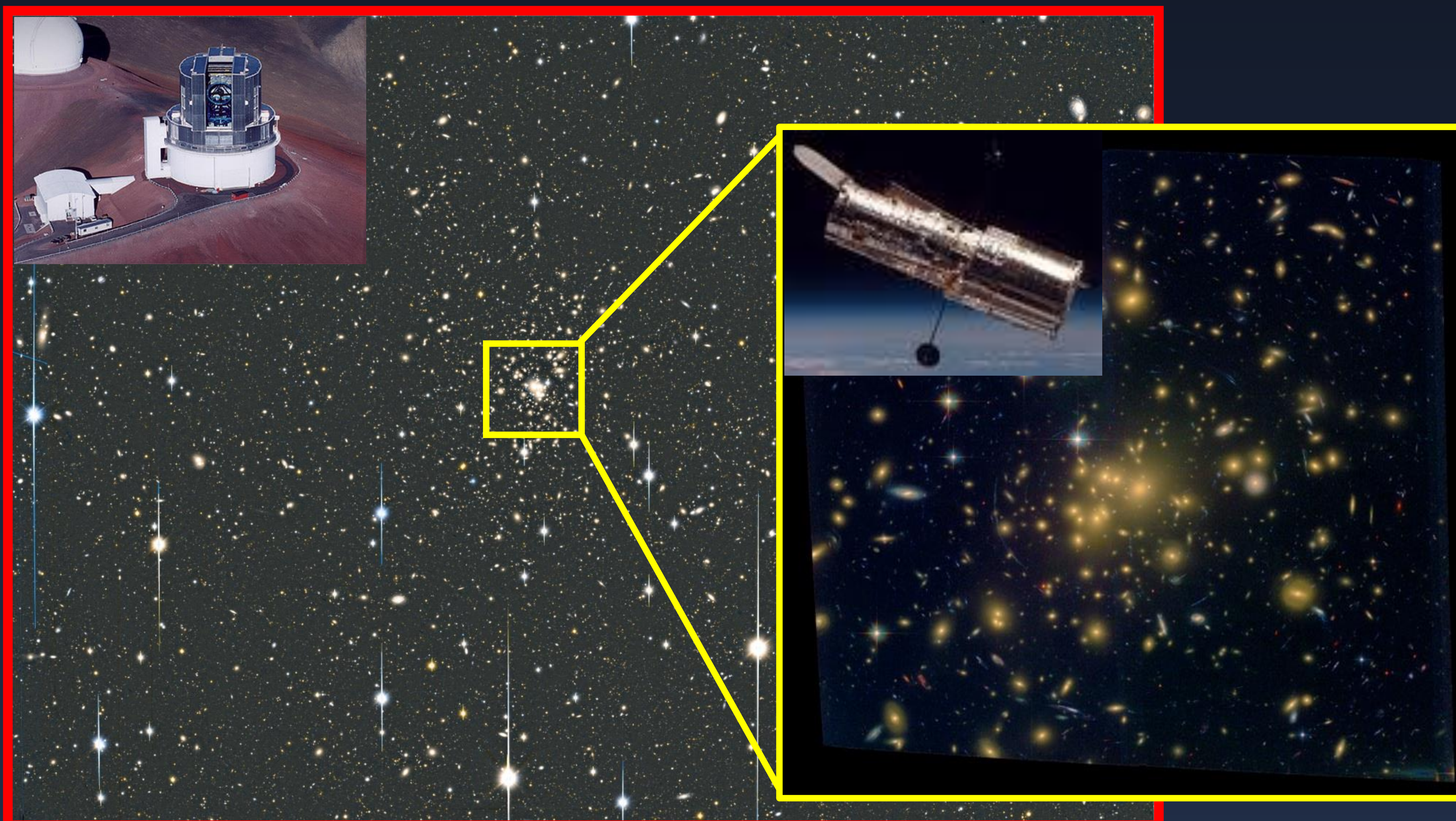

34 arcmin

Umetsu et al. 2016, *ApJ*, 821, 116

Cluster sample and data

- 20 CLASH clusters
  - $0.18 < z < 0.69$
  - $5 < M_{200c}/10^{14}M_{sun} < 30$
- M_s, r_s
  - Marginalized posteriors of NFW (M_{200c}, c_{200c}) from weak+strong lensing (Umetsu+16)
  - $<r_s>$ ~ 500kpc
- T_X
  - Core-excised *Chandra* temperature T(50-500kpc) (Donahue+14)
  - $<T_x>$ ~ 8keV

Cluster	z	r_s (kpc)	r_{200} (kpc)	M_s ($10^{14}\,M_\odot$)	M_{200} ($10^{14}\,M_\odot$)	T_X (keV)
Abell 383	0.187	304^{+159}_{-97}	1800^{+209}_{-189}	$1.4^{+1.0}_{-0.5}$	$7.9^{+3.1}_{-2.2}$	6.5 ± 0.24
Abell 209	0.206	834^{+243}_{-192}	2238^{+161}_{-172}	$5.2^{+2.2}_{-1.6}$	$15.4^{+3.6}_{-3.3}$	7.3 ± 0.54
Abell 2261	0.224	682^{+232}_{-170}	2542^{+192}_{-188}	$5.8^{+2.7}_{-1.8}$	$22.9^{+5.6}_{-4.7}$	7.6 ± 0.30
RX J2129.7+0005	0.234	294^{+133}_{-89}	1626^{+163}_{-154}	$1.1^{+0.7}_{-0.4}$	$6.1^{+2.0}_{-1.6}$	5.8 ± 0.40
Abell 611	0.288	560^{+250}_{-172}	2189^{+204}_{-208}	$3.8^{+2.3}_{-1.5}$	$15.6^{+4.8}_{-4.0}$	7.9 ± 0.35
MS 2137-2353	0.313	784^{+557}_{-357}	2064^{+261}_{-286}	$4.7^{+5.2}_{-2.6}$	$13.4^{+5.8}_{-4.9}$	5.9 ± 0.30
RX J2248.7-4431	0.348	643^{+422}_{-246}	2267^{+282}_{-261}	$4.9^{+4.8}_{-2.3}$	$18.5^{+7.8}_{-5.7}$	12.4 ± 0.60
MACS J1115.9+0129	0.352	738^{+249}_{-196}	2186^{+161}_{-174}	$5.1^{+2.4}_{-1.7}$	$16.6^{+4.0}_{-3.7}$	8.0 ± 0.40
MACS J1931.8-2635	0.352	501^{+441}_{-221}	2114^{+355}_{-311}	$3.5^{+4.6}_{-1.8}$	$15.0^{+8.9}_{-5.7}$	6.7 ± 0.40
RX J1532.9+3021	0.363	293^{+433}_{-114}	1544^{+191}_{-210}	$1.2^{+1.6}_{-0.5}$	$5.9^{+2.5}_{-2.1}$	5.5 ± 0.40
MACS J1720.3+3536	0.391	505^{+248}_{-162}	2055^{+204}_{-204}	$3.4^{+2.3}_{-1.4}$	$14.4^{+4.7}_{-3.9}$	6.6 ± 0.40
MACS J0416.1-2403	0.396	642^{+201}_{-156}	1860^{+146}_{-154}	$3.4^{+1.5}_{-1.1}$	$10.7^{+2.7}_{-2.4}$	7.5 ± 0.80
MACS J0429.6-0253	0.399	394^{+238}_{-143}	1792^{+225}_{-208}	$2.1^{+1.8}_{-0.9}$	$9.6^{+4.1}_{-3.0}$	6.0 ± 0.44
MACS J1206.2-0847	0.440	587^{+248}_{-176}	2181^{+165}_{-178}	$4.6^{+2.4}_{-1.7}$	$18.1^{+4.4}_{-4.1}$	10.8 ± 0.60
MACS J0329.7-0211	0.450	254^{+95}_{-63}	1697^{+129}_{-127}	$1.4^{+0.6}_{-0.4}$	$8.6^{+2.1}_{-1.8}$	8.0 ± 0.50
RX J1347.5-1145	0.451	840^{+339}_{-239}	2684^{+226}_{-230}	$9.8^{+5.6}_{-3.6}$	$34.2^{+9.4}_{-8.1}$	15.5 ± 0.60
MACS J1149.5+2223	0.544	1108^{+404}_{-291}	2334^{+169}_{-178}	$10.8^{+5.4}_{-3.7}$	$25.0^{+5.8}_{-5.3}$	8.7 ± 0.90
MACS J0717.5+3745	0.548	1300^{+347}_{-271}	2387^{+154}_{-165}	$13.2^{+5.3}_{-3.9}$	$26.8^{+5.6}_{-5.2}$	12.5 ± 0.70
MACS J0647.7+7015	0.584	468^{+254}_{-160}	1884^{+189}_{-192}	$3.3^{+2.3}_{-1.3}$	$13.7^{+4.6}_{-3.8}$	13.3 ± 1.80
MACS J0744.9+3927	0.686	574^{+269}_{-192}	1982^{+179}_{-185}	$4.9^{+3.1}_{-2.0}$	$17.9^{+5.3}_{-4.6}$	8.9 ± 0.80

Results: Principal Component Analysis

A fundamental plane (FP) exists in DM-baryon parameter space with 0.045dex (10%) scatter!

→ T_X is tightly coupled with (r_s, M_s)

$$a\log(r_s)+b\log(M_s)+c\log(T_X)=\text{const.}$$

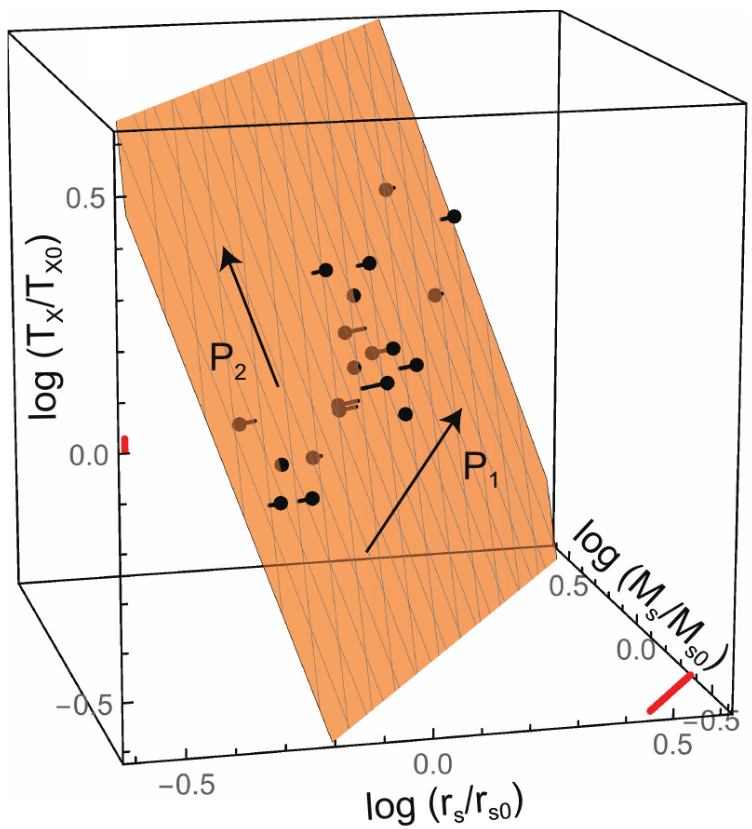

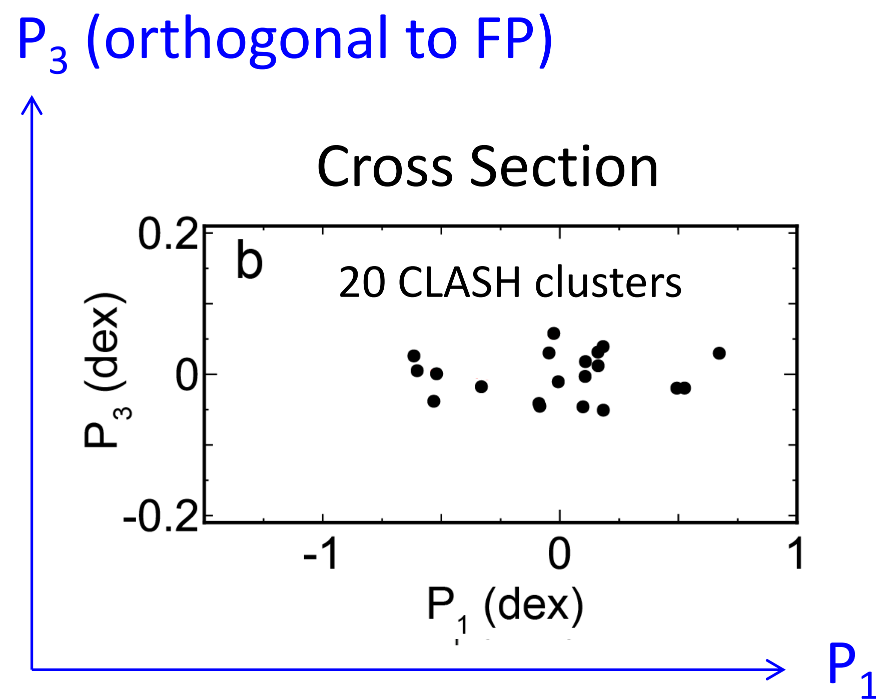

Fujita, Umetsu+18a

Plane Angle

The observed plane is significantly tilted from the canonical "virial" expectation, $T_X \propto M_s/r_s$

Direction of the plane normal: P_3

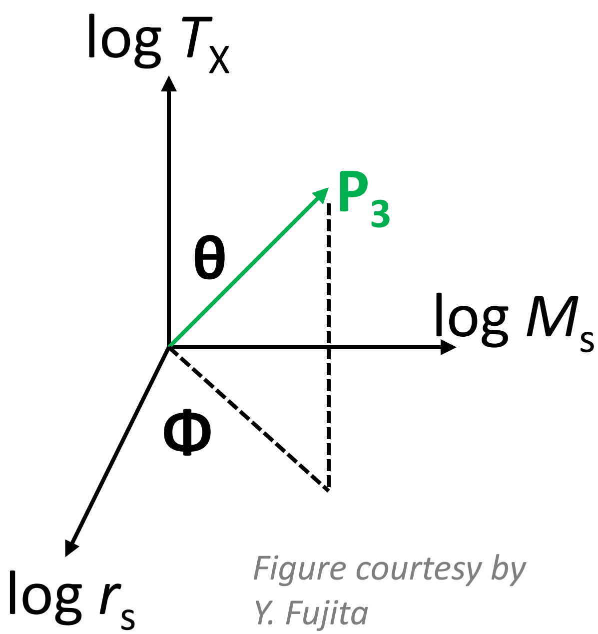

Figure courtesy by Y. Fujita

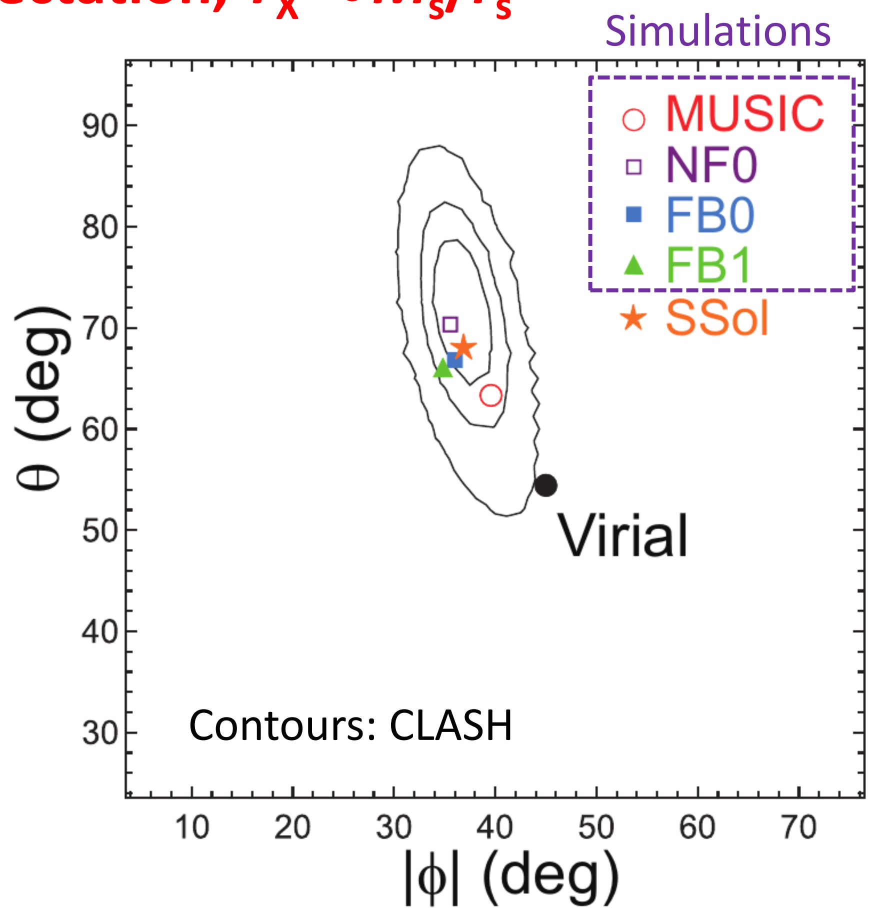

Fujita, Umetsu+18a

N-body + hydro Simulations

- Our sample is relatively small (N = 20)
  - Checks for selection bias (e.g., relaxation state) needed
  - Interpret data within the framework of ΛCDM
- **Adiabatic simulations**
  - 402 mass-selected halos with $M > 2\text{x}10^{14} M_{sun}/h$ from Meneghetti et al. (2014)
    - MUSIC: z=0.25
- **Radiative cooling + feedback (AGN/SNe) simulations**
  - 29 cluster halos with $M = (1\text{-}30)\text{x}10^{14} M_{sun}/h$ from Rasia et al. (2015)
    - FB0: z=0
    - NF0: z=0, adiabatic for comparison
    - FB1: z=1

Fujita, Umetsu+18a

(1) Adiabatic simulations

- Simulated cluster halos form a tight plane (0.025dex)!
  - The angle is consistent with the data
- The plane formed by most unrelaxed halos is almost the same as that of most relaxed halos, but with an increased scatter
- Selection bias due to the degree of relaxation is not significant

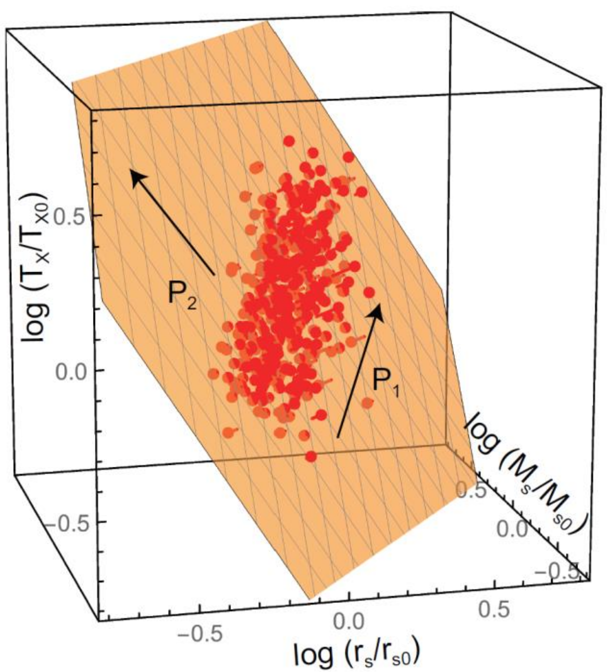

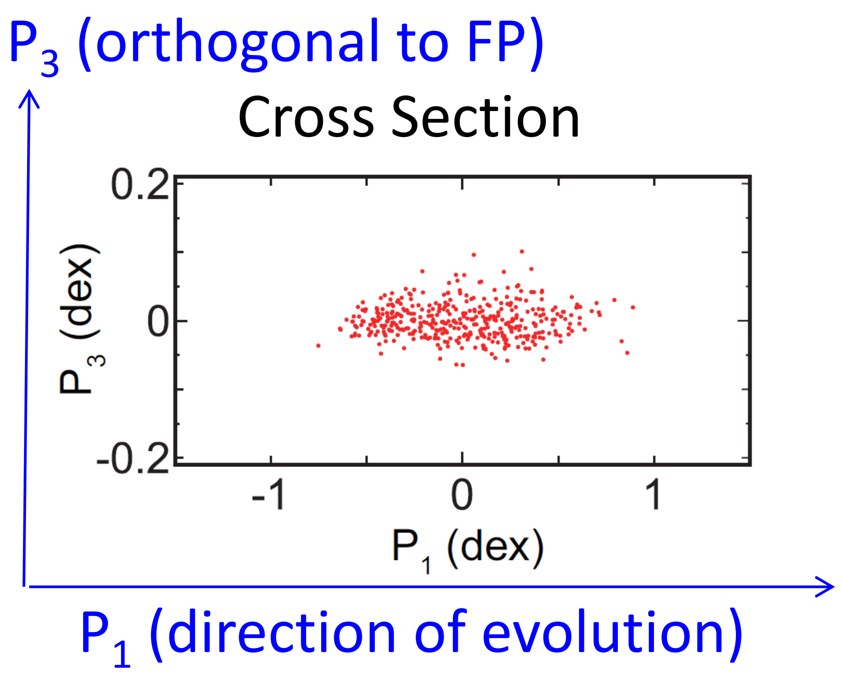

(2) Radiative cooling + feedback simulations

- The angle is consistent with the data
- FB0 plane is almost the same as NF0 (adiabatic) plane
  - The effects of cooling and feedback are not important at r_s ~ 500kpc
- FB1(z=1) and FB0(z=0) halos lie on the same plane (0.037dex)
  - Clusters evolve within the plane along the direction of P_1

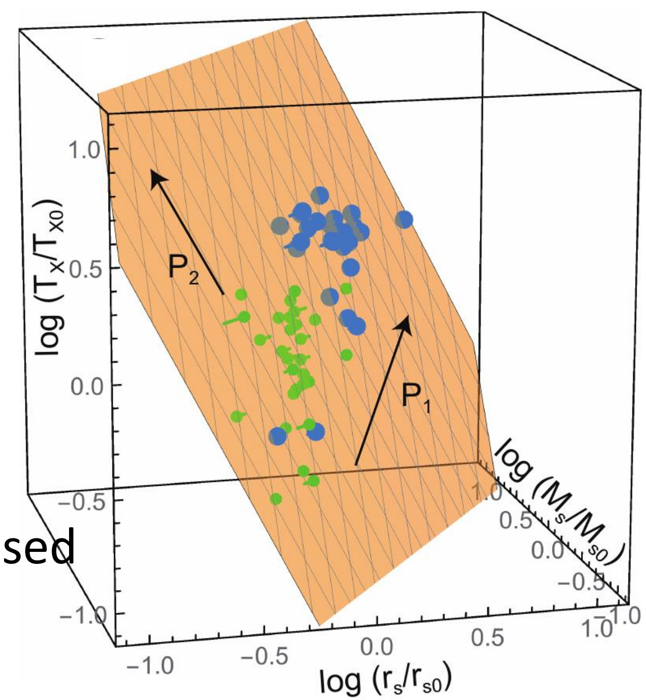

Core-excised
T used

P_3 (orthogonal to FP)

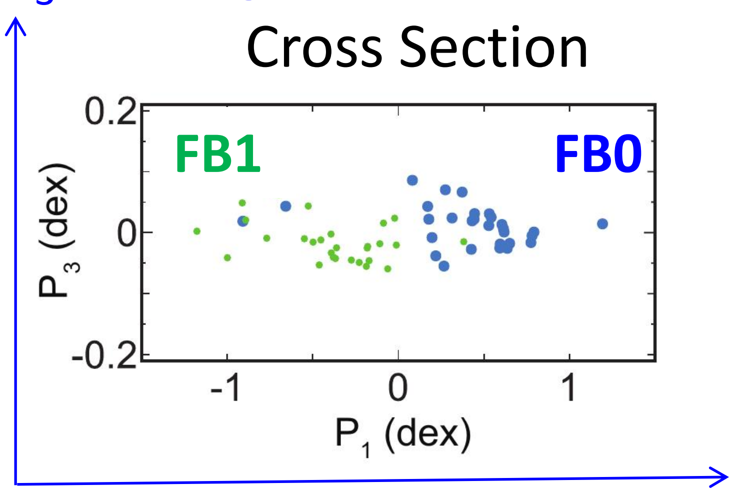

P_1 (direction of evolution)

What’s the physics governing FP?

A possible explanation: **Bertschinger (1985) secondary-infall similarity solution** for accretion of gas in a matter-dominant universe

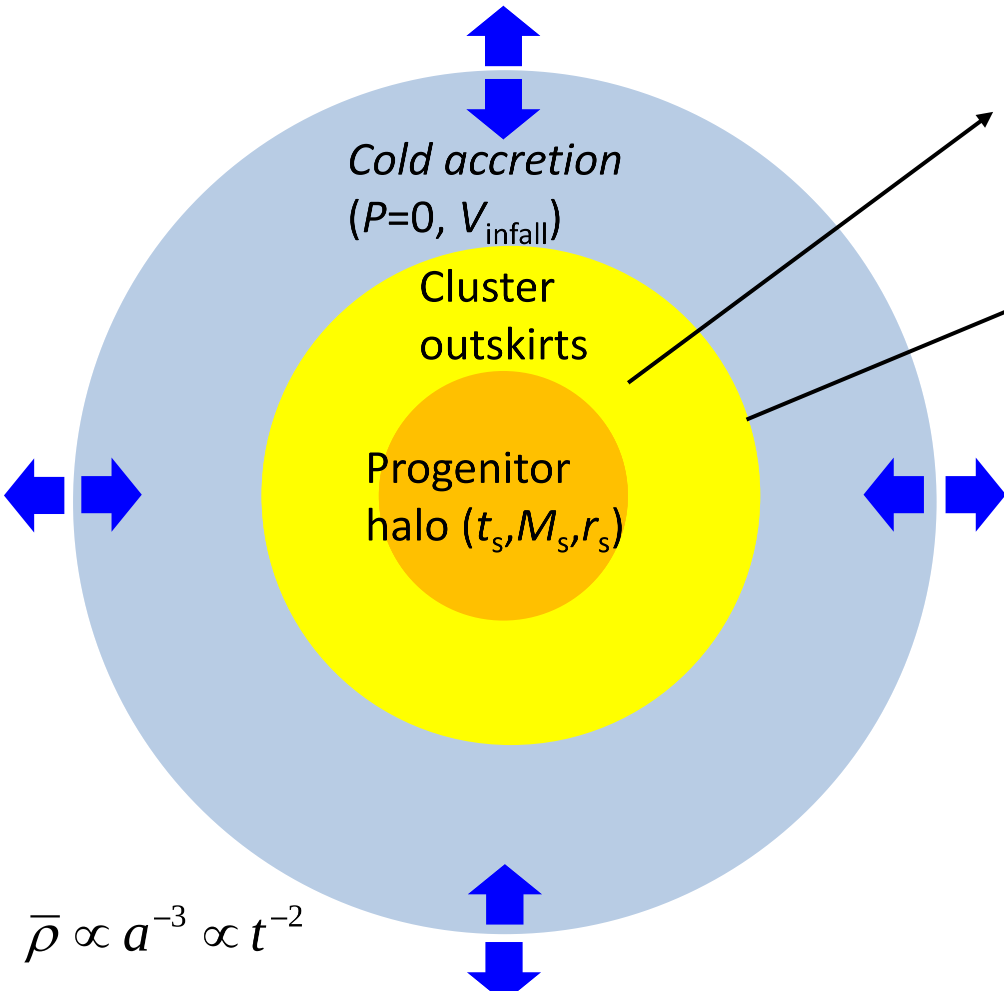

Shock-heated ideal gas, $P \propto \rho^{5/3}$

Accretion shock radius (shock jump conditions satisfied)

Dimensionless radial profiles

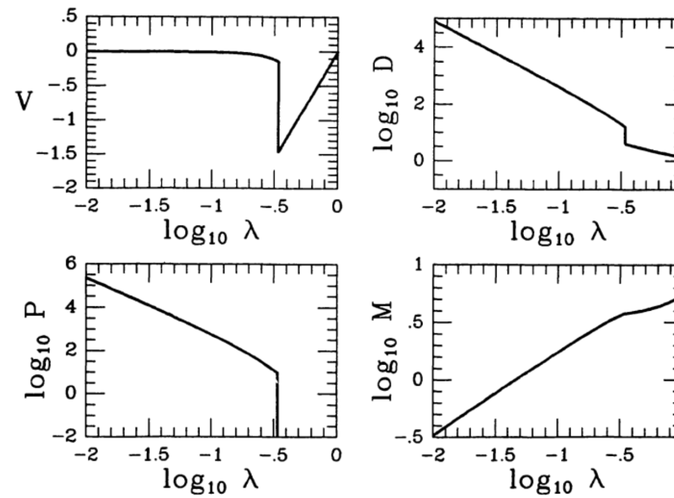

$\bar{\rho} \propto a^{-3} \propto t^{-2}$

What's the physics governing FP?

A possible explanation: Bertschinger (1985) secondary-infall similarity solution for accretion of gas in a matter-dominant universe

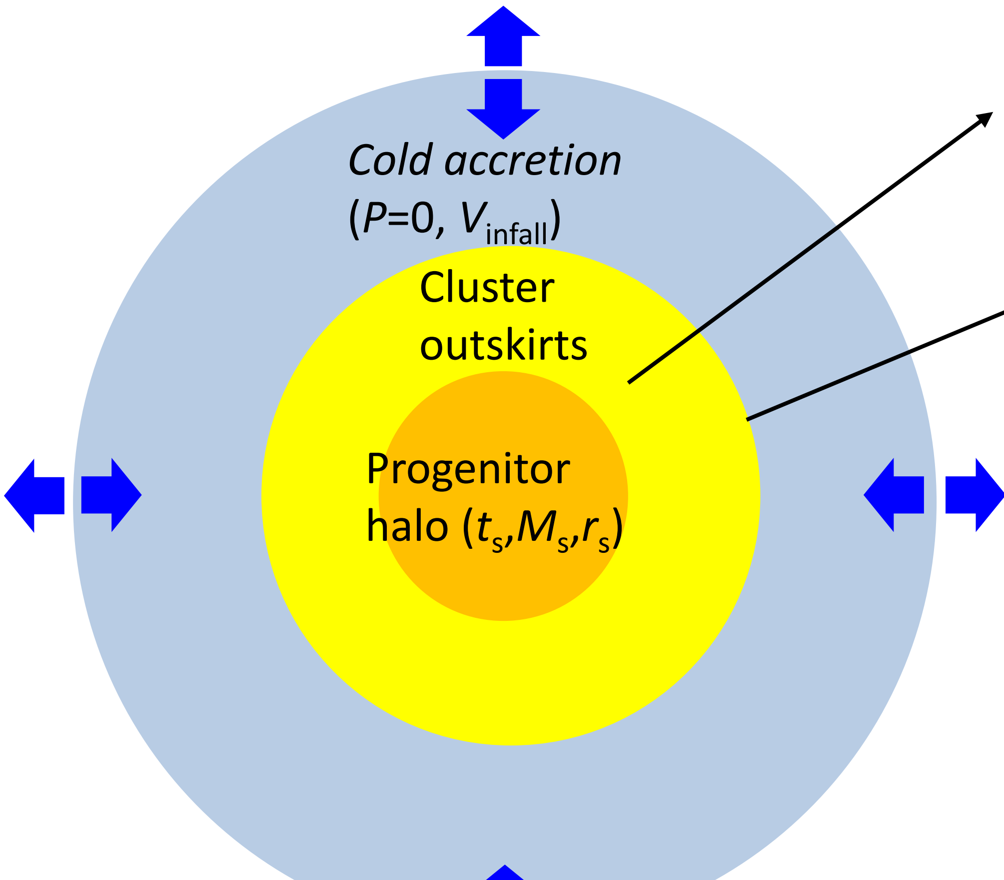

Shock-heated ideal gas, $P \propto \rho^{5/3}$

Accretion shock radius (shock jump conditions satisfied)

(1) Entropy integral of B85

(2) $P(k) \propto k^{-2}$ at cluster scales

→ (1)+(2) yield

$$T \propto \frac{M^{1.5}}{r^2}, \;\; r \propto M^{1/2}$$

$$@\, r = r_{\mathrm{s}}$$

$$\bar{\rho} \propto a^{-3} \propto t^{-2}$$

Fundamental Plane vs. Similarity Solution

Similarity solution (SSol)

$$r_s^{\ 2} M_s^{\ -(n+11)/6} T = \text{const.}$$

$$n \equiv \frac{d \ln P}{d \ln k} \approx \text{-}2 \ @ \ \text{cluster scales}$$

- The predicted angle (SSol) is consistent with observations and simulations
- In this picture, clusters are continuously evolving and growing with time
  - Momentum flux from matter accretion
  - Not in "virial" equilibrium $\frac{1}{2}\langle \ddot{I} \rangle = 2T - |W| - S \approx 0$
  - Gas in pressure equilibrium

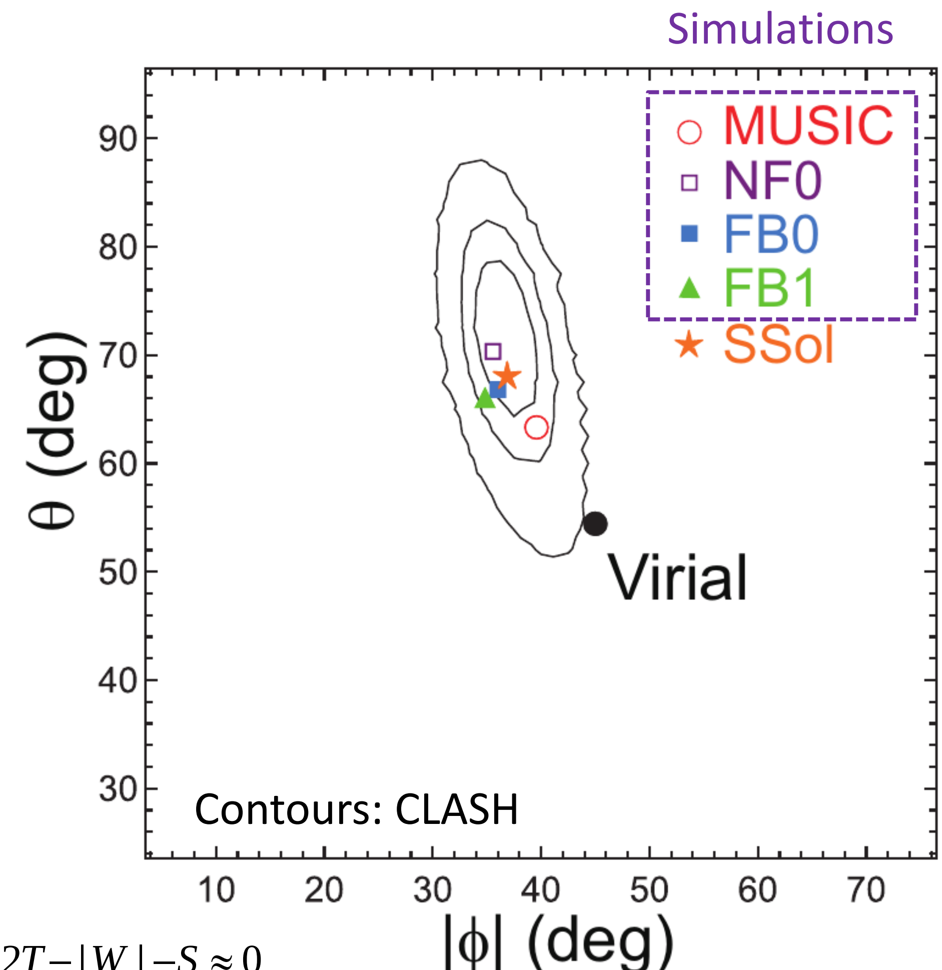

Fujita, Umetsu+18a

Stability of FP against mergers

Evolutionary track of a typical halo in the FB0+FB1 sample

- Clusters evolve along P_1
- T and (M_s,r_s) are tightly coupled and co-evolve
- Even during major ergers (A, B, E), the halo stays in the plane
  - T and (M_s,r_s) are anti-correlated
  - Mergers contributing to the thickness of the FP

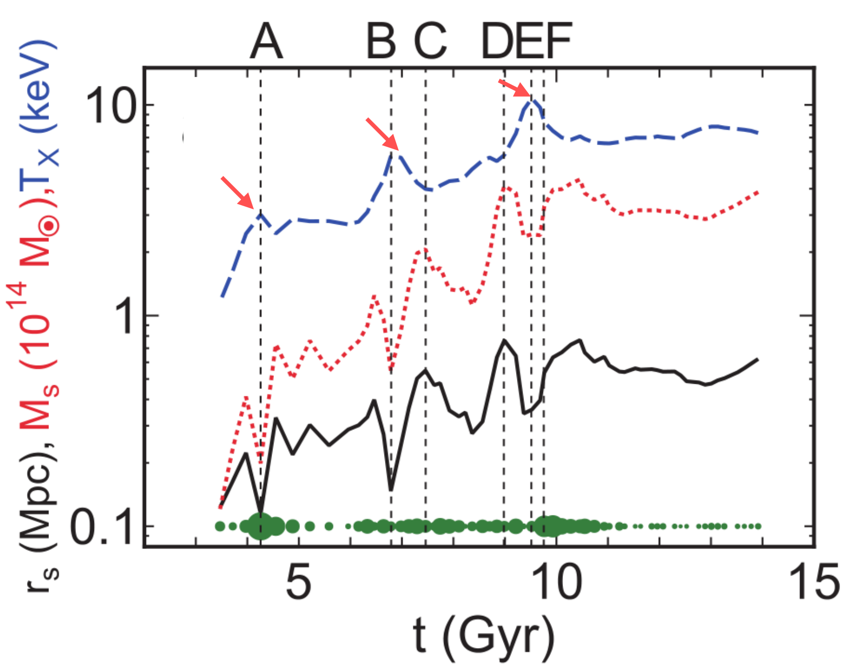

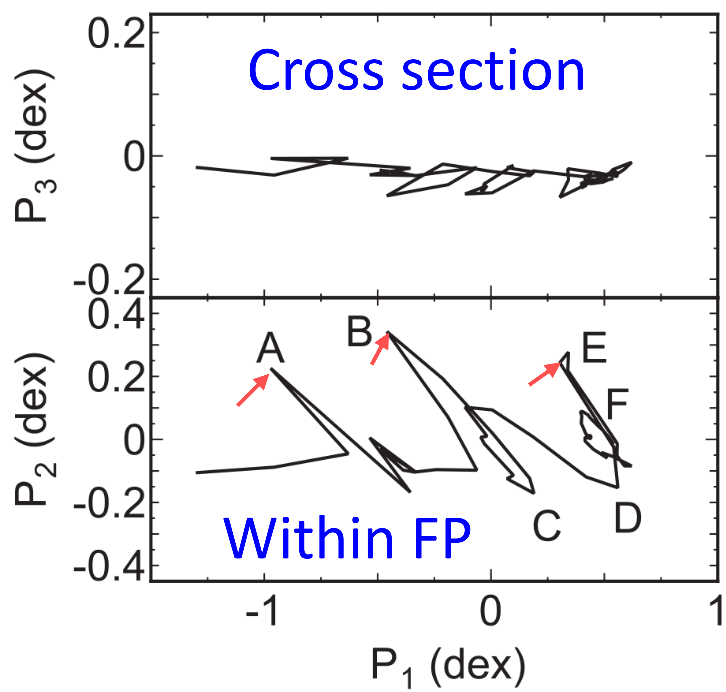

Application: cluster mass calibration

Calibrating X-ray hydrostatic mass estimates using the "shift" of the FP (Fujita, Umetsu et al. 2018b)

Red: 20 CLASH clusters
Black: 44 clusters from Ettori+10 (XMM-Newton)

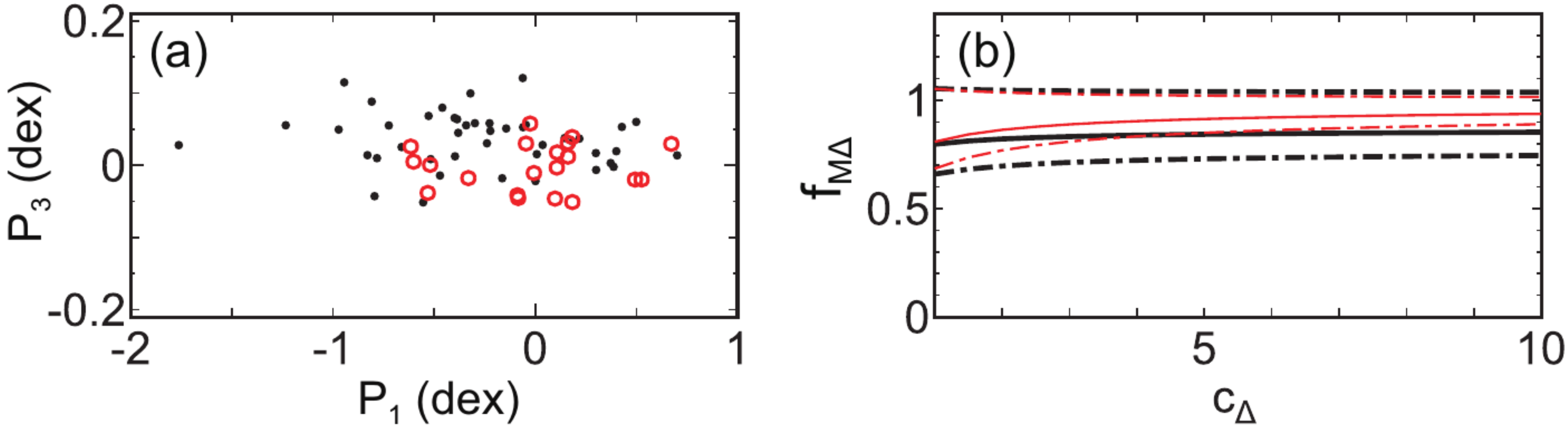

Mass calibration weakly depends on concentration c_Δ of the target sample

$f_M = M_{X\text{-}FP}/M_{FP}$ = 0.85+/-0.20, consistent with the expected level of HS bias (10-15%)

Summary

1. Observed clusters form a tight plane in DM-baryon parameter space (r_s, M_s, T).

2. The observed plane is significantly tilted from the virial expectation, $T \propto M_s/r_s$, and can be explained by a similarity solution (Bertschinger 1985):

   - Cluster outskirts are evolving with time through continuous mass accretion.
   - The Bertschinger 85 picture works for adiabatic gas + collisionless DM (e.g., Shi 2016).

3. Numerical simulations reproduce the observed plane, independently of the gas physics implemented in the code.

4. Cluster halos are predicted to evolve within the plane along the direction of P1:

   - The plane is stable even against major mergers!!!

5. See Paper II (Fujita, Umetsu+18b) for further applications: e.g., cluster mass calibration, origin of the *M*-*T* relation

Supplemental slides

A close look at simulated clusters

Similarity solution: $r_s \propto M_s^{1/2}$ ($r_s \propto M_s^{1/1.65}$ by Zhao+09)

Formation epoch of halos $\rho_{\rm crit}(t_{\rm f}) \sim \dfrac{M_{\rm s}}{r_{\rm s}^3} \equiv \rho_s$

The self-similar solution predicts $r_s \propto M_s^{1/2}$ for cluster-scale halos ($P(k) \sim k^{-2}$), which is consistent with the direction of cluster evolution (P_1) found from our observations and simulations

Cluster evolution depends on the initial matter power spectrum $P(k) \sim k^n$

FP projected on r_s-M_s

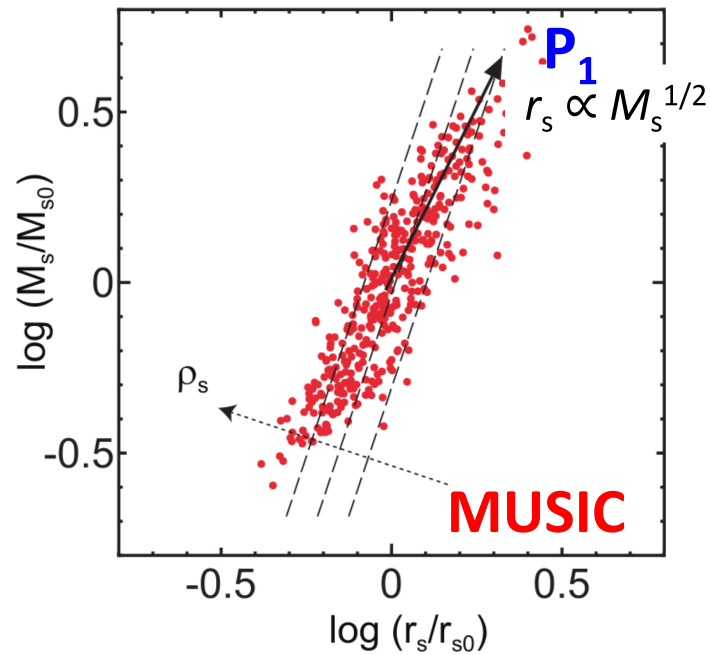

Fujita, Umetsu+18

Weak lensing: shear & magnification

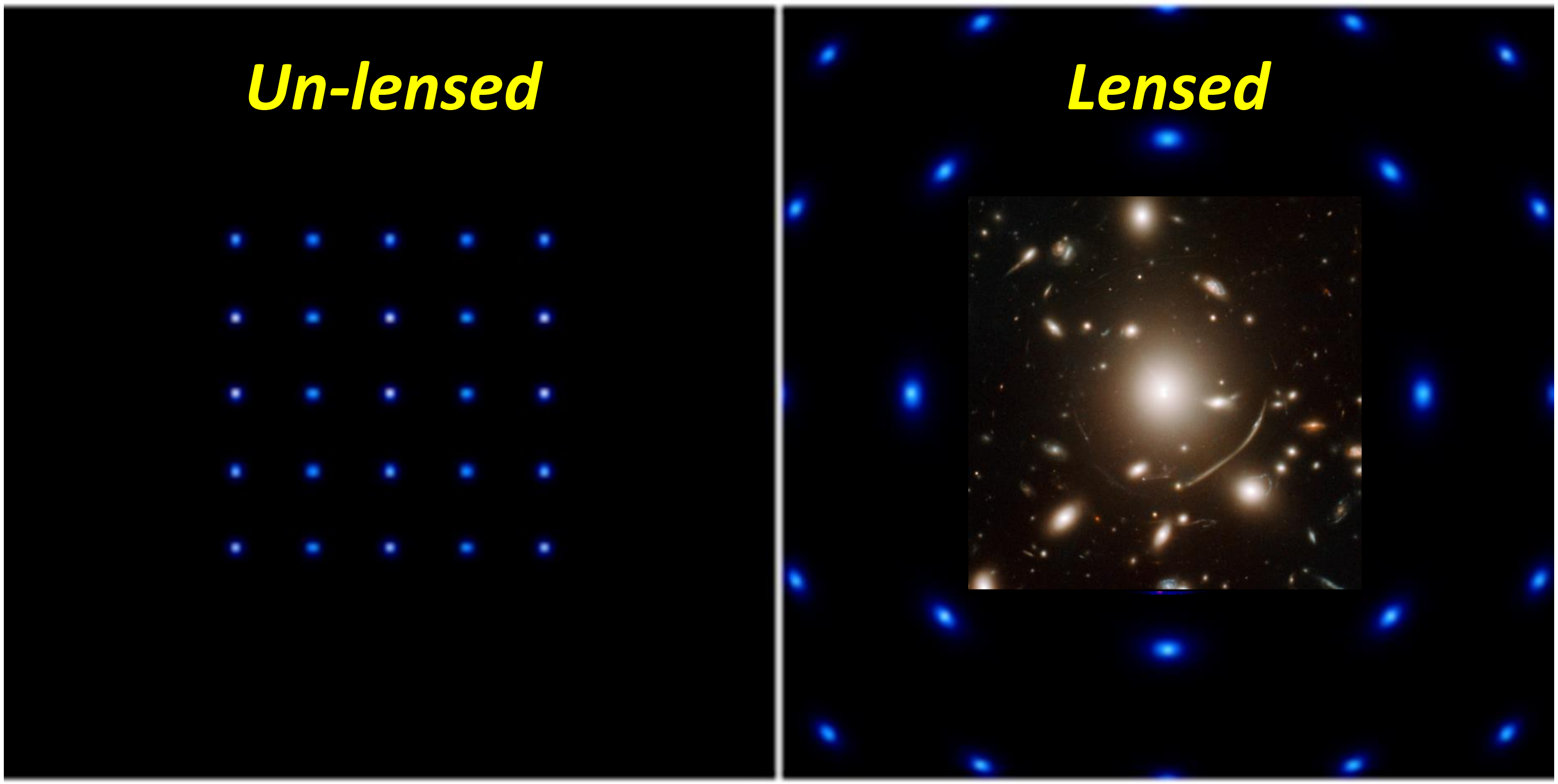

- **Shear** (Kaiser 92)
  - ✓ Shape distortion: $\delta e \sim \gamma$
- **Magnification** (Broadhurst+95)
  - ✓ Flux amplification: μF
  - ✓ Area distortion: $\mu \Delta \Omega$

Sensitive to "differential" matter density

$$\Sigma_c \gamma_+ = \Delta\Sigma(R) \equiv \Sigma(<R) - \Sigma(R)$$

Sensitive to "total" matter density

$$\mu \approx 1 + 2\kappa; \quad \Sigma_c \kappa = \Sigma(R) = \int (\rho - \bar{\rho}_m) dl$$

Cluster sample and data

- 20 CLASH clusters
  - $0.18 < z < 0.69$
  - $4 < M_{200c}/10^{14} M_{sun}/h < 20$
  - 16 X-ray regular clusters
  - 4 high-magnification lenses
- M_s, r_s
  - Marginalized posteriors of NFW (M_{200c}, c_{200c}) from weak+strong lensing (Umetsu+16)
- T_X
  - Core-excised *Chandra* temperature T(50-500kpc) (Donahue+14)

Cluster	z	r_s (kpc)	r_{200} (kpc)	M_s ($10^{14}\ M_\odot$)	M_{200} ($10^{14}\ M_\odot$)	T_X (keV)
Abell 383	0.187	304^{+159}_{-97}	1800^{+209}_{-189}	$1.4^{+1.0}_{-0.5}$	$7.9^{+3.1}_{-2.2}$	6.5 ± 0.24
Abell 209	0.206	834^{+243}_{-192}	2238^{+161}_{-172}	$5.2^{+2.2}_{-1.6}$	$15.4^{+3.6}_{-3.3}$	7.3 ± 0.54
Abell 2261	0.224	682^{+232}_{-170}	2542^{+192}_{-188}	$5.8^{+2.7}_{-1.8}$	$22.9^{+5.6}_{-4.7}$	7.6 ± 0.30
RX J2129.7+0005	0.234	294^{+133}_{-89}	1626^{+163}_{-154}	$1.1^{+0.7}_{-0.4}$	$6.1^{+2.0}_{-1.6}$	5.8 ± 0.40
Abell 611	0.288	560^{+250}_{-172}	2189^{+204}_{-208}	$3.8^{+2.3}_{-1.5}$	$15.6^{+4.8}_{-4.0}$	7.9 ± 0.35
MS 2137-2353	0.313	784^{+557}_{-357}	2064^{+261}_{-286}	$4.7^{+5.2}_{-2.6}$	$13.4^{+5.8}_{-4.9}$	5.9 ± 0.30
RX J2248.7-4431	0.348	643^{+422}_{-246}	2267^{+282}_{-261}	$4.9^{+4.8}_{-2.3}$	$18.5^{+7.8}_{-5.7}$	12.4 ± 0.60
MACS J1115.9+0129	0.352	738^{+249}_{-196}	2186^{+161}_{-174}	$5.1^{+2.4}_{-1.7}$	$16.6^{+4.0}_{-3.7}$	8.0 ± 0.40
MACS J1931.8-2635	0.352	501^{+441}_{-221}	2114^{+355}_{-311}	$3.5^{+4.6}_{-1.8}$	$15.0^{+8.9}_{-5.7}$	6.7 ± 0.40
RX J1532.9+3021	0.363	293^{+433}_{-114}	1544^{+191}_{-210}	$1.2^{+1.6}_{-0.5}$	$5.9^{+2.5}_{-2.1}$	5.5 ± 0.40
MACS J1720.3+3536	0.391	505^{+248}_{-162}	2055^{+204}_{-204}	$3.4^{+2.3}_{-1.4}$	$14.4^{+4.7}_{-3.9}$	6.6 ± 0.40
MACS J0416.1-2403	0.396	642^{+201}_{-156}	1860^{+146}_{-154}	$3.4^{+1.5}_{-1.1}$	$10.7^{+2.7}_{-2.4}$	7.5 ± 0.80
MACS J0429.6-0253	0.399	394^{+238}_{-143}	1792^{+225}_{-208}	$2.1^{+1.8}_{-0.9}$	$9.6^{+4.1}_{-3.0}$	6.0 ± 0.44
MACS J1206.2-0847	0.440	587^{+248}_{-176}	2181^{+165}_{-178}	$4.6^{+2.4}_{-1.7}$	$18.1^{+4.4}_{-4.1}$	10.8 ± 0.60
MACS J0329.7-0211	0.450	254^{+95}_{-63}	1697^{+129}_{-127}	$1.4^{+0.6}_{-0.4}$	$8.6^{+2.1}_{-1.8}$	8.0 ± 0.50
RX J1347.5-1145	0.451	840^{+339}_{-239}	2684^{+226}_{-230}	$9.8^{+5.6}_{-3.6}$	$34.2^{+9.4}_{-8.1}$	15.5 ± 0.60
MACS J1149.5+2223	0.544	1108^{+404}_{-291}	2334^{+169}_{-178}	$10.8^{+5.4}_{-3.7}$	$25.0^{+5.8}_{-5.3}$	8.7 ± 0.90
MACS J0717.5+3745	0.548	1300^{+347}_{-271}	2387^{+154}_{-165}	$13.2^{+5.3}_{-3.9}$	$26.8^{+5.6}_{-5.2}$	12.5 ± 0.70
MACS J0647.7+7015	0.584	468^{+254}_{-160}	1884^{+189}_{-192}	$3.3^{+2.3}_{-1.3}$	$13.7^{+4.6}_{-3.8}$	13.3 ± 1.80
MACS J0744.9+3927	0.686	574^{+269}_{-192}	1982^{+179}_{-185}	$4.9^{+3.1}_{-2.0}$	$17.9^{+5.3}_{-4.6}$	8.9 ± 0.80

Fujita, Umetsu+18

A close look at simulated clusters

Similarity solution: $r_s \propto M_s^{1/2}$ ($r_s \propto M_s^{1/1.65}$ by Zhao+09)

Formation epoch of halos $\rho_{\rm crit}(t_{\rm f}) \sim \frac{M_{\rm s}}{r_{\rm s}^3} \equiv \rho_s$

The self-similar solution predicts $r_s \propto M_s^{1/2}$ for cluster-scale halos ($P(k) \sim k^{-2}$), which is consistent with the direction of cluster evolution (P_1) found from our observations and simulations

Cluster evolution depends on the initial matter power spectrum $P(k) \sim k^n$

FP projected on r_s-M_s

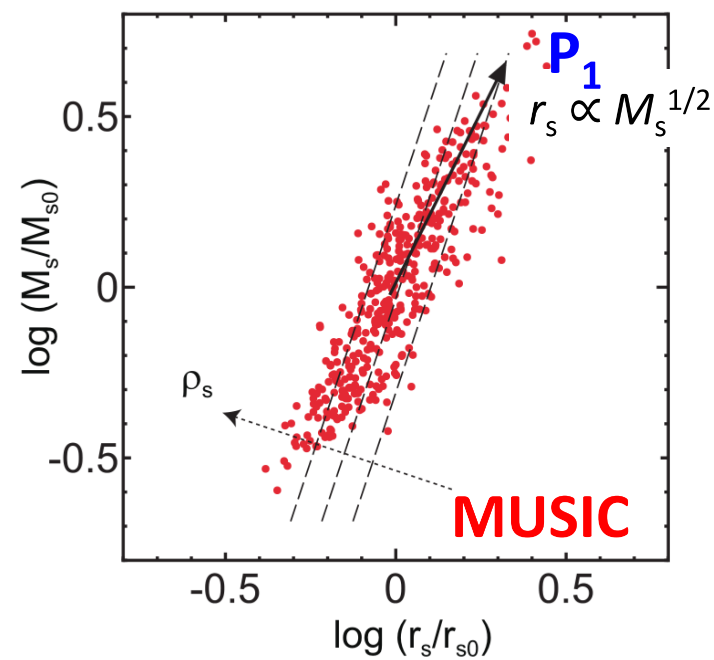

Fujita, Umetsu+18

NFW vs. Similarity solution

NFW profile (DM)

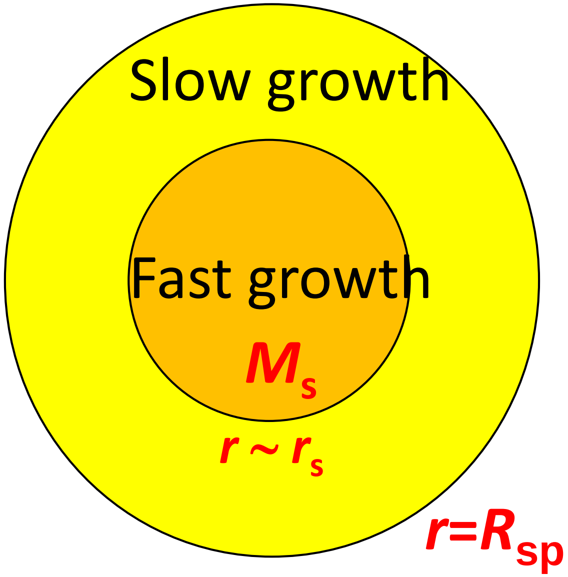

Similarity solution (ICM)

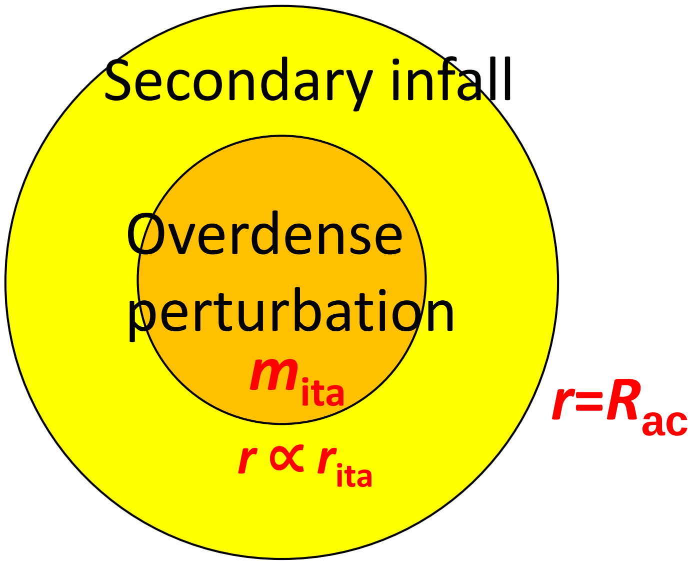

Projections of simulated clusters

Halos evolve with $r_s \propto M_s^{1/2}$ ($r_s \propto M_s^{1/1.65}$ by Zhao+09)

Formation epoch of halos $\rho_{\rm crit}(t_{\rm f}) \sim \frac{M_{\rm s}}{r_{\rm s}^3}$

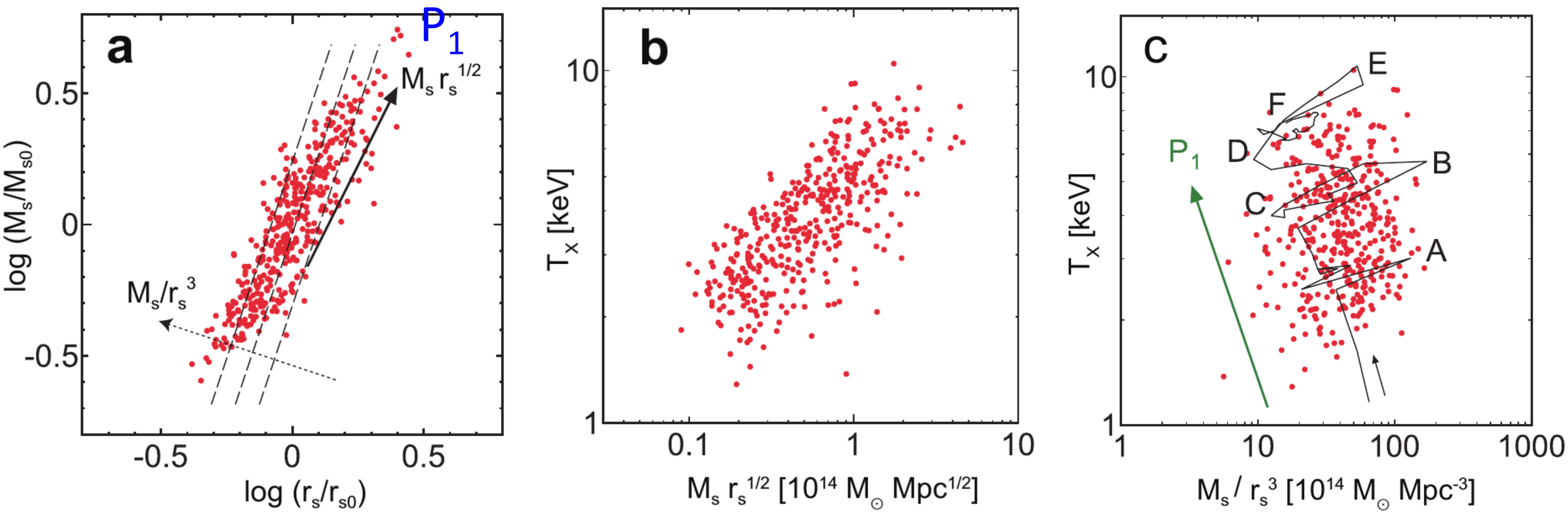

MUSIC cosmological simulations (DM + adiabatic gas)

Fujita, Umetsu+18

Gravitational Shear

$$\gamma = \partial\partial\Psi / 2$$

$$\partial := e^{i\phi}\partial_r$$

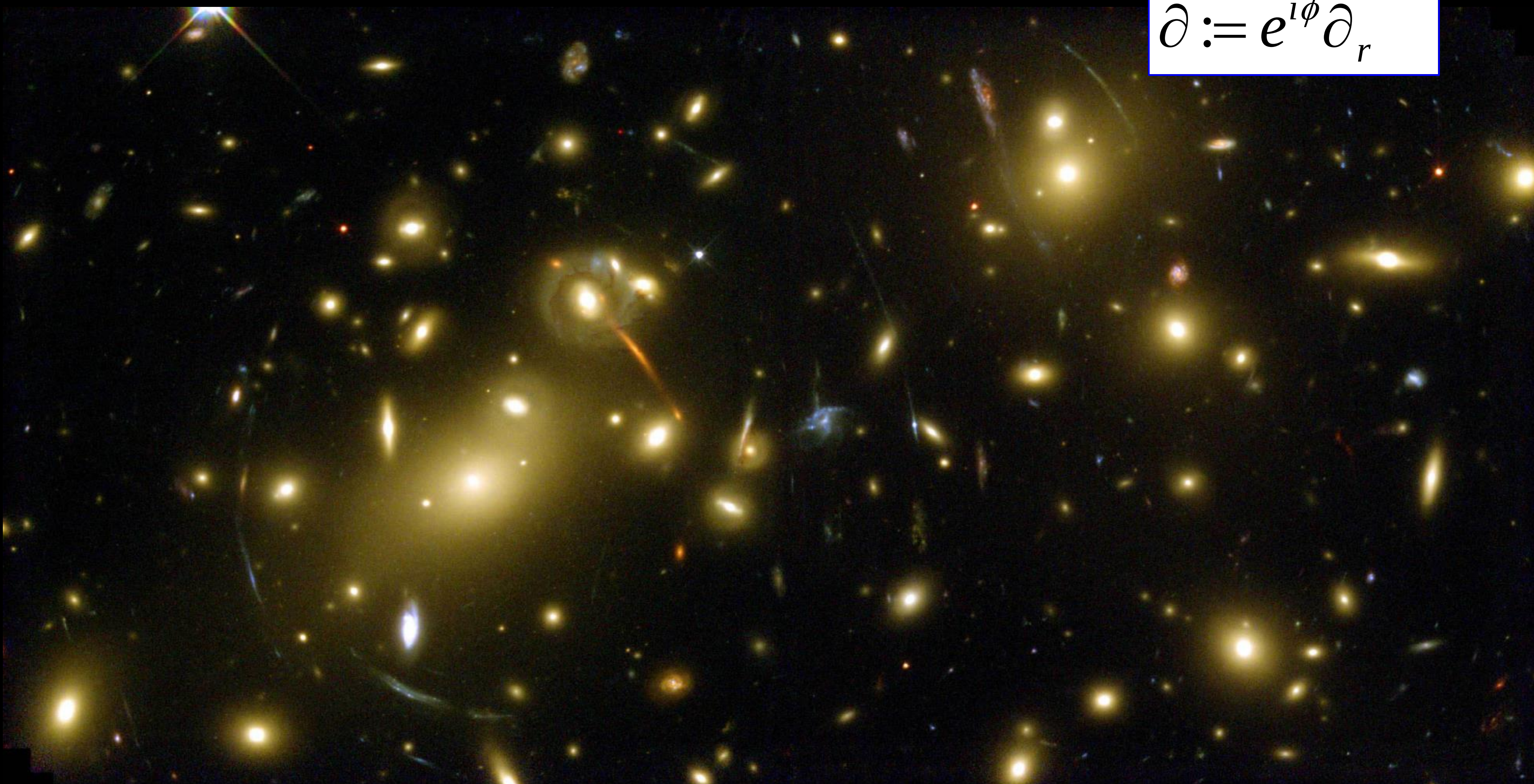

Gravitational Magnification

$$\kappa = \partial\partial^{*}\Psi / 2 = \Delta\Psi / 2$$

$$\partial := e^{i\phi}\partial_{r}$$

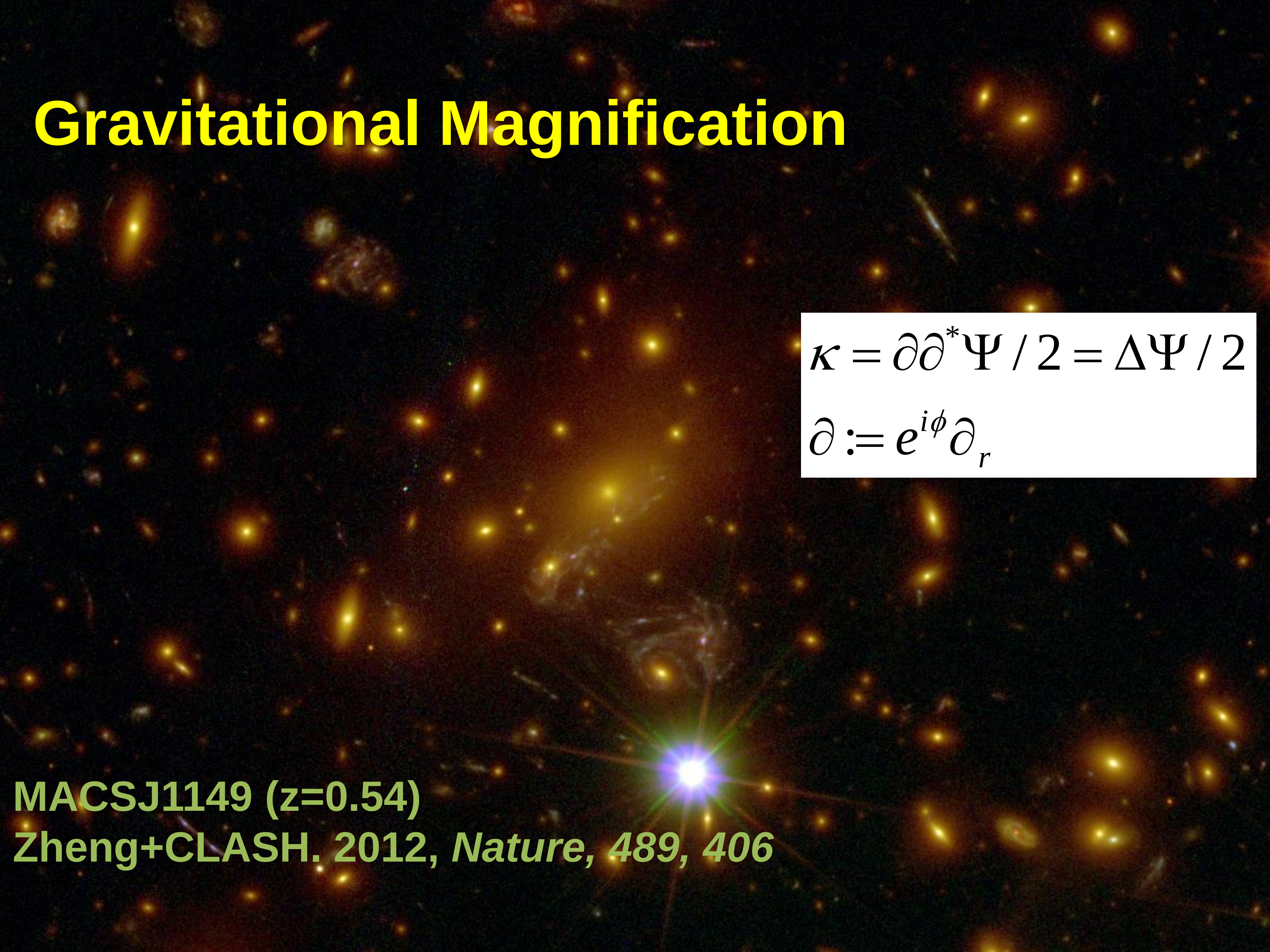

MACSJ1149 (z=0.54)
Zheng+CLASH. 2012, *Nature, 489, 406*